To suppress tin whisker growth by using (100)-oriented copper

Lin, Han-Wen; Lu, Jia-Ling; Hu, Chih-Chia; Tu, K. N.; Chen, Chih

Published in:
Journal of Materials Research and Technology

Published: 01/03/2025

Document Version:
Final Published version, also known as Publisher's PDF, Publisher's Final version or Version of Record

Published version (DOI):
10.1016/j.jmrt.2025.02.021

Publication details:
Lin, H.-W., Lu, J.-L., Hu, C.-C., Tu, K. N., & Chen, C. (2025). To suppress tin whisker growth by using (100)-oriented copper. *Journal of Materials Research and Technology*, *35*, 3217-3225. https://doi.org/10.1016/j.jmrt.2025.02.021

Journal of Materials Research and Technology 35 (2025) 3217–3225

Contents lists available at ScienceDirect

Journal of Materials Research and Technology

journal homepage: www.elsevier.com/locate/jmrt

To suppress tin whisker growth by using (100)-oriented copper

Han-Wen Lin [a], Jia-Ling Lu [a], Chih-Chia Hu [a], K.N. Tu [b,c], Chih Chen [a,*]

[a] Department of Materials Science and Engineering, National Yang Ming Chiao Tung University, Hsinchu, 300093, Taiwan
[b] Department of Materials Science and Engineering, City University of Hong Kong, Hong Kong
[c] Department of Electrical Engineering, City University of Hong Kong, Hong Kong

ARTICLE INFO

Handling editor: SN Monteiro

ABSTRACT

Effect of Cu crystallographic orientations on the Sn whisker growth is investigated in this study. Three types of Cu under-layer (randomly, <111>, <100>-oriented) were prepared for electroplating of pure Sn. After 672 h of room temperature (RT) storage, a lot of whiskers were found on the Sn surface electroplated on the randomly-oriented Cu, whereas very few whiskers can be seen on those electroplated on the <111>– or the <100>-oriented Cu. It is also found that the behavior of intermetallic compound (IMC) growth at the Sn–Cu interface is quite different between the randomly- and specifically-oriented Cu films, which leads to divergent phenomena of Sn whisker growth. Furthermore, after 7944 h of RT storage, both the <111>– and the <100>-oriented Cu films are proven to be effective on preventing Sn whisker growth. Orientation analysis indicated the Sn grains on the <111>– and the <100>-oriented Cu possesses <110> preferred orientation, which may slow down the formation of the Cu–Sn IMCs.

1. Introduction

In 1940s, Compton et al. [1] in The Bell Telephone Laboratories found Sn whiskers on the surface finish of electronic components as they tried to replace cadmium with pure Sn. Ever since then, a great deal of effort has been spent to investigate the spontaneous growth of Sn whiskers [2,3]. Generally, whisker growth refers to the formation of thin, hair-like protrusions, typically from Sn in electronic components. These whiskers can grow spontaneously from metal surfaces over time, especially in environments with mechanical stress, temperature fluctuations, or high humidity. Sn whisker growth, driven by a compressive stress gradient, can occur even at room temperature (RT). These whiskers are known to form spontaneously on Sn finishes applied to Cu surfaces. With the widespread use of Pb-free Sn-rich solders on Cu conductors in consumer electronics, Sn whisker growth has become a significant reliability concern. NASA reported that the Sn whiskers may cause failure of satellites [4]. However, the growth mechanism still remains controversial. Some scientists suggest that whisker formation is due to recrystallization or abnormal grain growth [5–8], while others think that it involves atomic migration caused by internal stress gradient [9–13]. Recently, much evidence emerges, and it shows that the formation of whiskers is accompanied with stress relief in Sn films [14–19]. The formation of metal whiskers is believed to result from the energy gain associated with the electrostatic polarization of metal filaments in an electric field, which is described by the so-called electrostatic theory of whisker growth [20–25]. This field is generated by surface imperfections such as contamination, oxide layers, and grain boundaries. Zhang et al. [26] and Tang et al. [27] reported that intense whiskers grew as Ti_2SnC decomposed, which is attributed to that Sn atoms released from mechanochemically decomposed Ti_2SnC have high chemical potential and spontaneous crystallization occurs. Therefore, nowadays, people are more convinced that the compressive stress gradient inside the Sn layer should be responsible for Sn whiskers growth [28,29]. The oxide layer on the Sn whisker surface plays a critical rule too.

Despite the arguments over the growth mechanism, the method to prevent Sn whiskers growth from electrical components shows little variation. Researchers offered several effective ways to mitigate Sn whiskers, such as heat treatment, underlayers, and altering plating solution [8,30]. In a review paper, Tu [10] concluded that a post-annealing can effectively prevent whiskers from forming on the Sn–Cu films. Lee and Lee [11] also found that the near-zero stress state exists in their cantilever experiments after the Sn layer was annealed at 150 °C for 2 h. Annealing is also helpful to form an intermetallic barrier layer. Fukuda et al. found that an annealing treatment at 100–180 °C for 30 min or more will produce a diffusion barrier layer of intermetallic

* Corresponding author.
E-mail address: chihchen@nycu.edu.tw (C. Chen).

https://doi.org/10.1016/j.jmrt.2025.02.021
Received 27 September 2024; Received in revised form 31 January 2025; Accepted 3 February 2025
Available online 4 February 2025

compounds (IMCs) [31]. Therefore, another way to impede whisker formation is to introduce a diffusion barrier between Cu and Sn [32–37]. Although some studies use organic compounds as a buffer layer [38], Ni is always considered to be a good candidate. In 1978, Hada et al. published a study, indicating that a Ni underlayer of 2 μm or more is effective to hinder Sn whisker formation [39]. Other studies also provide more supported materials to their conclusion by comparing whisker growth for Sn layers deposited on Cu with and without a Ni intermediate layer [40–42]. In the perspective of altering plating solution, reports claimed that organic additive can control surface morphology of electroplated Sn layer and reduce possible nucleation sites for Sn whiskers. Organic additive also possesses a controlling effect on the preferred orientation of Sn layer, leading to a favorable microstructure for whisker inhibition.

No doubt, after decades of efforts, there are many reported techniques to control Sn whisker growth [30,42–48]. However, most of them focused on either providing an efficient diffusion barrier, addition of impurities in solders, or controlling properties of the Sn layer. Hashim et al. [42] reported that adding Ni in Sn-0.7Cu solder can suppress the Sn whisker formation. Illés et al. [43] proposed that Sn whiskers can be mitigated by the addition of TiO_2 and ZnO nano-particles. Hsiao et al. [49] adopted single crystalline Cu substrates with different orientations, and they found the orientation of Cu has a strong effect on the morphologies and orientation of Cu–Sn IMCs. However, how the morphologies of Cu–Sn IMCs affect the Sn whisker orientation is still unknown. Only a few studies presented the effect of Cu composition and IMC orientation on the relief of Sn whiskers formation [50,51]. In particular, to the best of our knowledge, there is no literature addressing the effecting of Cu orientation on the Sn whisker formation.

We report here an approach for diminishing Sn whisker growth based on specifically-oriented Cu films. Both <111>− and <100>-oriented Cu films were served as substrates, which were covered by electroplated Sn layers with fixed thickness. After RT storage tests, the effect of specifically-oriented Cu films on retardation of whisker formation is revealed by surface morphology observation and cross-sectional examination.

2. Experimental

In this research, diffusion couples of pure Sn and Cu were prepared by electroplating. A 20-nm thick seed layer of Cu was sputtered on the silicon wafer with 200 nm of TiW adhesion layer. Then, an electroplating procedure deposited Cu layers on silicon chips. With varied parameters, such as additives, current density, or stirring rate, the microstructure of Cu can be controlled. In this case, we produced <111>-oriented Cu (<111> Cu) with nano-twins as well as randomly-oriented Cu (RO-Cu). The <111>-oriented Cu film was further annealed at 450 °C for 30 min to change its preferred orientation to <100>, which is denoted as <100> Cu in this paper. In the same time, the Cu grains also grew rapidly. With the afore-mentioned steps, the Cu substrates were properly prepared for Sn whisker growth study. All the procedures and experiment settings are documented in the previous studies [52–55]. It is noteworthy to state that the surface roughness for both the <111>-and <100>-oriented Cu films should have no obvious differences, because the <100>-oriented Cu film was the annealed specimen from the <111>-oriented Cu film [54]. For each substrate, pure Sn films were electroplated on the Cu films with the same settings. A Sn plate with 99.9% purity was chosen to be the anode metal. The electrolyte was the commercial solution with cations of Sn^{2+}. The current density is 20 mA/cm^2. The thickness of the electroplated Cu and Sn films were ~5 μm. Orientation maps were collected by an energy dispersive X-ray spectroscopy (EDAX) electron back-scattered diffraction (EBSD) system within the scanning electron microscope (JEOL 7001 FE-SEM). The images and the polished cross-sections were taken by the FEI Nova 200 Nanolab Dualbeam FIB.

3. Results and discussion

In Fig. 1, the orientation maps of the three Cu substrates are shown along with the reference color-coding. Black lines are used to identify the boundaries in the microstructure. Fig. 1(a), (b) and (c) are correspondingly the orientation maps of the Cu substrates used in this study. All grains in Fig. 1(a) were blue, and those in Fig. 1(b) were red. As the color coding of Fig. 1(d) inferred, these two Cu substrates were <111>− and <100>-oriented. Many different colors are shown in Fig. 1(c), which indicates that it was randomly-oriented. The grain size of these substrates was also varied. On the average, the grain size of <111>-oriented Cu was 1.04 μm, and those of the randomly-oriented one was 3.14 μm. Much bigger grains existed on the <100>-oriented Cu because it was annealed at 450 °C, leading to extremely anisotropic grain growth [54]. The grain size of <100>-oriented Cu was 369.97 μm. It has been reported that the microstructural changes associate with abnormal grain growth in nanotwinned Cu (nt-Cu) during annealing [56,57]. As a thick nt-Cu film was annealed at 350 °C for 45 min, its microstructure shifted from <111>-oriented nanotwins to <100>-oriented grains, with an average grain size exceeding 100 μm. For nt-Cu films thicker than 5 μm, the transformation occurred at a lower temperature of 300 °C. We found a critical temperature for abnormal grain growth, where no microstructural changes take place, likely due to nucleation limitations. As nucleation occurs, the grain growth is highly anisotropic, with lateral growth at least an order of magnitude faster than normal (through-thickness) growth.

RT storage tests were conducted right after Sn layers were electroplated on each Cu substrate. The temperature of the air-conditioned room was around 25 °C, and the humidity was around 70%. The samples were kept in a plastic Petri dish covered with a lid. After varied duration of storage, samples were examined from the surface for whisker formation. Fig. 2 shows the surface morphology for each Sn–Cu diffusion couple after 672 and 1200 h of storage. These electron images were collected while samples were tilted to give more prominence to whisker formation. In Fig. 2(a)–(c), surface morphology of Sn layers on RO-Cu, <111> Cu and <100> Cu films, respectively, was revealed after 672 h of storage. It was noticeable that some observable whiskers already existed on the Sn layer with the RO-Cu as the under-layer. Meanwhile, there were no visible extrusions on the Sn layer with <111>− and <100> Cu as the under-layer. When we extended the storage time, the difference was more obvious. Electron images with a higher magnification after 1200-h storage are shown in Fig. 2(d)–(f). In Fig. 2(d), lots of whiskers extruded out from the surface of the Sn layer electroplated on the RO-Cu film. Like many whiskers reported in other studies, these filament-like metal extrusions had some stripes on their surface. Some of them were bent or kinked. In Fig. 2(e) and (f), Sn layers with <111>− and <100>-oriented Cu underlays are shown. Obviously, Sn whiskers were barely found on them. In fact, we did find some tiny extrusions on the Sn layers with <111>-oriented Cu as underlayer. They are marked with white circle in Fig. 2(e). As it shows, the number of whiskers was much less, and these whiskers were much smaller in both diameter and length compared with those grown on the randomly-oriented Cu film. However, the Sn layer on <100>-oriented Cu films was whisker-free as Fig. 2(f) exhibits.

Fig. 3 shows the surface morphology of Sn layers after RT storage for 2376 and 7944 h. In this Figure, a larger area was examined to provide a general impression for each Sn layer. In Fig. 3(a), lots of tiny spots appeared on Sn. Each spot was a Sn whisker. In comparison, whiskers were hardly found in Fig. 2(b) and (c). It showed that both amount and size of whiskers are much less for these layers electroplated on the <111>− and <100>-oriented Cu films. After 7944 h of RT storage, there were some noticeable spots on the Sn layers with <111>-oriented Cu underlayer. However, compared to Fig. 3(d), it is still a great improvement on mitigating whisker formation. It should be noticed that these results were from samples kept for 11 months, which means the Sn layers on both <111>− and <100>-oriented Cu substrates had no

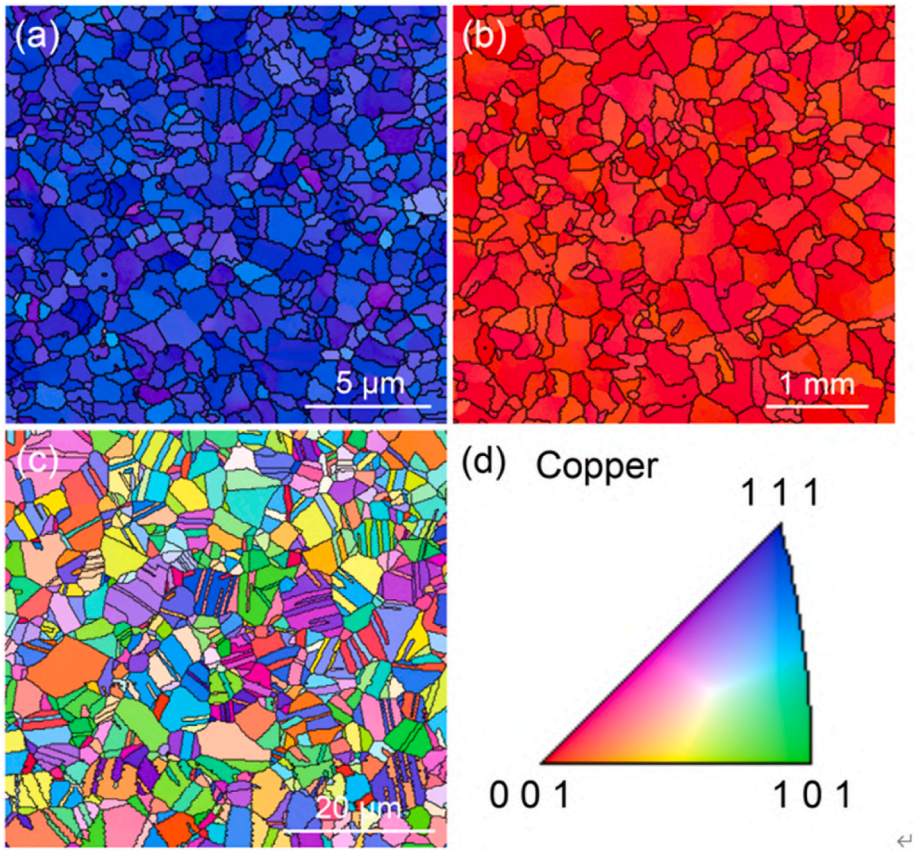

Fig. 1. The plan-view orientation maps of (a) <111>−, (b) <100>− and (c) randomly-oriented copper substrates; (d) The corresponding inverse pole figure.

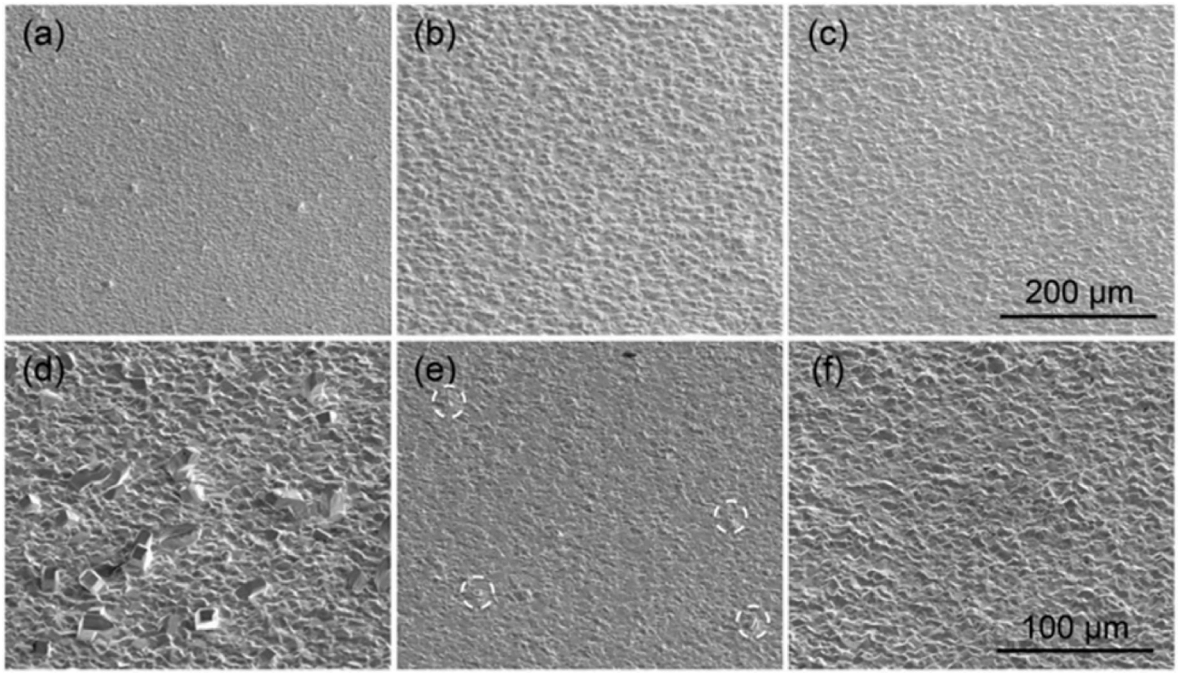

Fig. 2. Plan-view SEM images of Sn layers on (a) randomly-, (b) <111>−, (c) <100>-oriented Cu substrates after 672-h RT storage; Sn layers on (d) randomly-, (e) <111>−, (f) <100>-oriented Cu substrates after 1200-h RT storage. The electron microscopy tilt angles were 52°.

significant whisker formation for nearly one year. Meanwhile, for those pure Sn layers on ordinary Cu films, lots of Sn whiskers were growing from the surface.

In Table 1, we made a statistical analysis about the number of the whiskers on the observing area. For each sample, at different times, we took three different areas on our sample to make the calculation. Besides, for the Sn layers on <111>− and <100>-oriented Cu films, we counted whiskers with higher magnification, and every visible extrusion

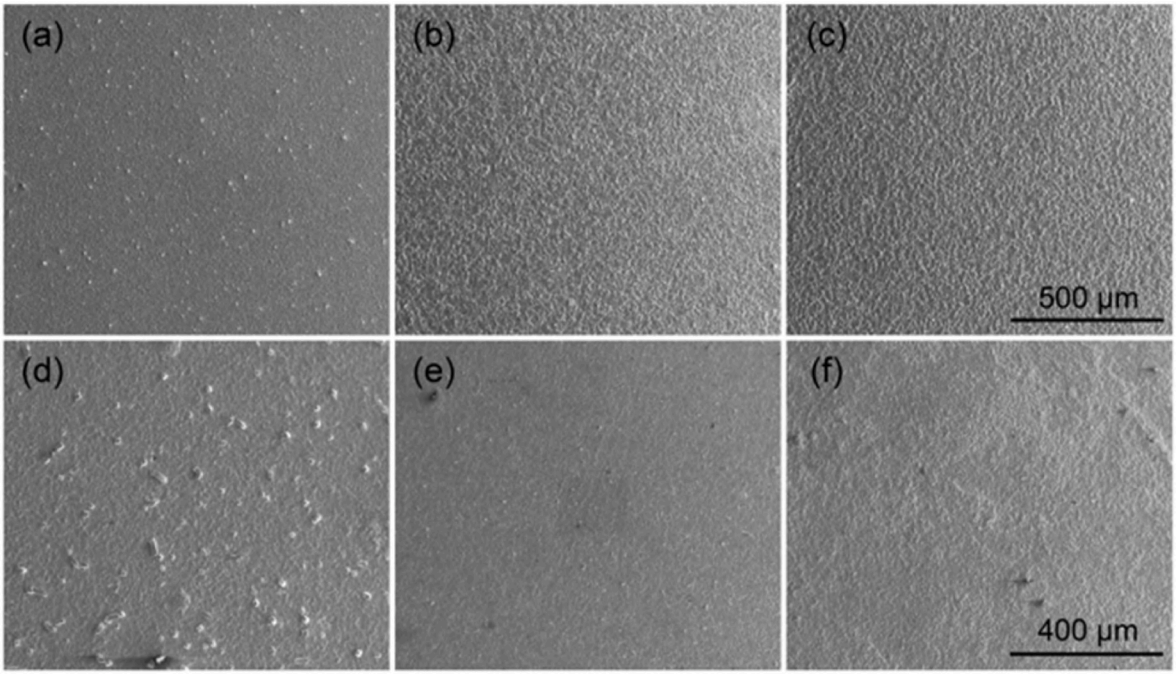

Fig. 3. Plan-view SEM images of Sn layers on (a) randomly-, (b) <111>−, (c) <100>-oriented Cu substrates after 2376-h RT storage; Sn layers on (d) randomly-, (e) <111>−, (f) <100>-oriented Cu substrates after 7944-h RT storage. The electron microscopy tilt angles were 0°.

Table 1
Whisker density (whiskers/cm^2) on different substrates after 2136 and 7944 h of RT storage (*2376 h).

Aging time	On RO-Cu	On <111> Cu	On <100> Cu
2136 h	194	32	0*
7944 h	198	175	10

was taken as a whisker. As this table shows, after 2136 h, there were 194 whiskers/cm^2 on the Sn layers with the randomly-oriented Cu substrates while there were only 32 whiskers/cm^2 on those Sn layers with <111>-oriented Cu substrates. There was no whisker found on the Sn layer with <100>-oriented Cu substrates after 2376-h storage. After 7944 h, there were 198, 175, and 10 whiskers/cm^2 on different Sn layers, respectively. For those layers on randomly-oriented Cu substrates, the whisker formation seemed to be stable. For the Sn layers on <111>-oriented Cu films, the number of whiskers increased significantly. However, those tiny extrusions were not comparable in size with those in Fig. 3(d) and (e) showed. The <100>-oriented Cu substrates were still effective on impediment to whisker formation. Only about 10 whiskers/cm^2 were found, and all of them were pretty small extrusions.

Just like the difference among all the surfaces of different samples,

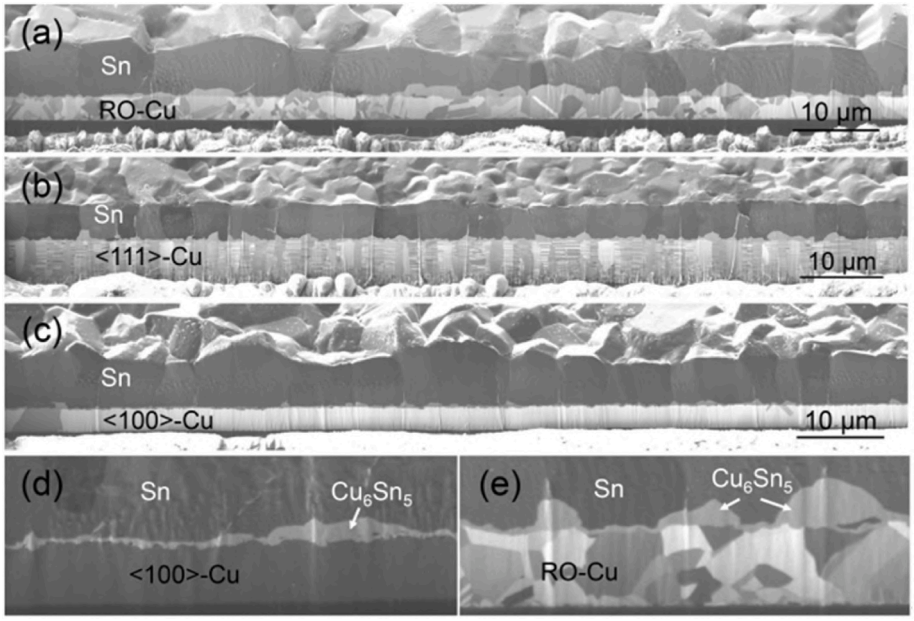

Fig. 4. The cross-sectional ion images of Cu–Sn couples on (a) randomly-, (b) <111>−, (c) <100>-oriented Cu substrates after 7944-h storage; the interface between Sn and (d) <100>− and (e) randomly-oriented Cu.

the interface between Cu and Sn also presented intriguing results. In Fig. 4, cross-sectional areas of Sn–Cu diffusion couples after 7944 h of storage are shown. These figures were taken with ion beam in the FIB. The contrast between grains was contributed by channeling of incident ions between lattice planes. The samples consisted of silicon chips, Cu substrates and Sn layers, as illustrated in Fig. 4. The diffusion couples composed of pure Sn and randomly-, <111>– and <100>-oriented Cu, are demonstrated in Fig. 4(a)–(c), respectively. It should be noted that there are layers of IMCs between the Cu and Sn. After analyzing them with EDS, they were confirmed to be the phase of Cu_6Sn_5. Although all the IMCs were the same from all the diffusion couples, there was a great difference about the appearance of them. In Fig. 4(a), the formation of the intermetallic was non-uniform. In some parts of the interface, there was only a thin layer of Cu_6Sn_5, which can be hardly observed. In other parts, the intermetallic formed as convex substance wedging in the Sn layer. The formation of Cu_6Sn_5 between Sn and <111>-oriented Cu was different. There was also uneven growth of the intermetallic, but the divergence between the thin layer and wedging parts is much smaller. Also, instead of being only a few larger IMCs, the wedging ones were more dispersed into several small parts on <111>-oriented Cu. In the diffusion couple made of pure Sn and <100>-oriented Cu, the formation of Cu_6Sn_5 between Cu and Sn was pretty uniform. Compared with those on the randomly- and <111>-oriented Cu, the intermetallic appeared to form evenly and cover the whole interface between Cu and Sn. In Fig. 4 (d) and (e), we showed the interface in a higher magnification. As compared in these Figures, the formation of Cu_6Sn_5 did exhibit great discrepancy. Rather flat Cu_6Sn_5 covered <100>-oriented Cu, while uneven ones lay on randomly-oriented Cu. It is also noteworthy to state that the Cu–Sn IMCs grew faster in the Sn grain boundaries, as seen in Fig. 4. Cu atoms may diffuse rapidly through Sn grain boundaries and form Cu–Sn IMCs in the grain boundaries, and impose compressing stress in the Sn grains, resulting in the growth of Sn whiskers [54].

The uneven growth of Cu–Sn intermetallic is regarded as one of the sources of compressive stress, especially for those formed on the grain boundaries of Sn [55]. To explain the effect of these IMCs, we have to consider the reaction between Cu and Sn as well as the diffusivity of Cu in Sn. We take the mole volume of Cu, Sn and Cu_6Sn_5 to be 7.32, 16.24, and 119.18 cm^3/mol [56,57], respectively. When Cu reacts with Sn, the chemical equation for the formation of Cu_6Sn_5 is $6Cu + 5Sn \rightarrow Cu_6Sn_5$. It takes 6 Cu atoms and 5 Sn atoms to form one Cu_6Sn_5 compound. The reaction leads to 4.75% volume shrinkage. It should not be responsible for the source of compressive stress. Nevertheless, for the intermetallic on randomly-oriented Cu, they formed mostly in grain boundaries of Sn layers in Fig. 4(e). As we know, the formation of Cu_6Sn_5 is a diffusion-controlled process [58,59]. Grain boundaries are always faster diffusion paths for atoms since they are not as densely-packed as the internal of grains, especially at lower temperatures. Therefore, at room temperature, the Cu atom would diffuse into grain boundaries of Sn and form Cu_6Sn_5 at the boundaries. That would give 46.77% volume increment, which leads to compressive stress inside the Sn grains. While wedge-shaped IMCs exert compressive stress to nearby areas, other parts or grains would remain as stress-free. This stress gradient would drive Sn atoms to diffuse, leading to Sn whisker formation.

In the case of <111>– and <100>-oriented Cu films as substrates, the uneven growth of intermetallic and the wedge-shaped Cu_6Sn_5 were remarkably reduced. As shown in Fig. 4(b), the number of Cu_6Sn_5 at the grain boundaries of Sn was more, but the size of them was smaller. It is helpful to distribute the compressive stress. As compressive stress was redistributed, the stress gradient could not be effective. Therefore, the whisker formation was delayed and mitigated. In the case of Sn layers with <100>-oriented Cu substrates, Cu_6Sn_5 tended to grow uniformly as shown in Fig. 4(c) and (d). When most of the intermetallic formed evenly at the interface between Cu and Sn, there would be much less compressive stress in the Sn layer. When the compressive stress was greatly reduced, a large stress gradient no longer existed, resulting in an effective way to relieve whisker formation.

Since the Cu–Sn IMCs may form in the Sn grain boundaries, as illustrated in Fig. 4(b) and in literature [54,57] further analysis on the Sn grain size and grain boundaries were performed. Fig. 5 shows the plan-view EBSD images on the Sn grain orientations for the three specimens. The preferred orientation for the Sn grains on RO-Cu is < 221>; whereas it is < 110> for Sn grains grown on <111> Cu and <100> Cu substrates. The difference in the Sn grain orientation may be another factor to affect the growth of Cu–Sn IMCs, and thus to influence the Sn whisker growth. In addition, the Sn grain size may be another factor to produce an effect on the Sn whisker growth. The distribution of Sn grain size is displayed in Fig. 6. The average grain size is 6.5 ± 3.1 μm, 5.7 ± 3.9 μm, and 7.4 ± 4.1 μm for the RO-Cu, <111> Cu and <100> Cu substrates, respectively. The grain size of the Sn grains on the three Cu substrates was controlled at the same level. The misorientation

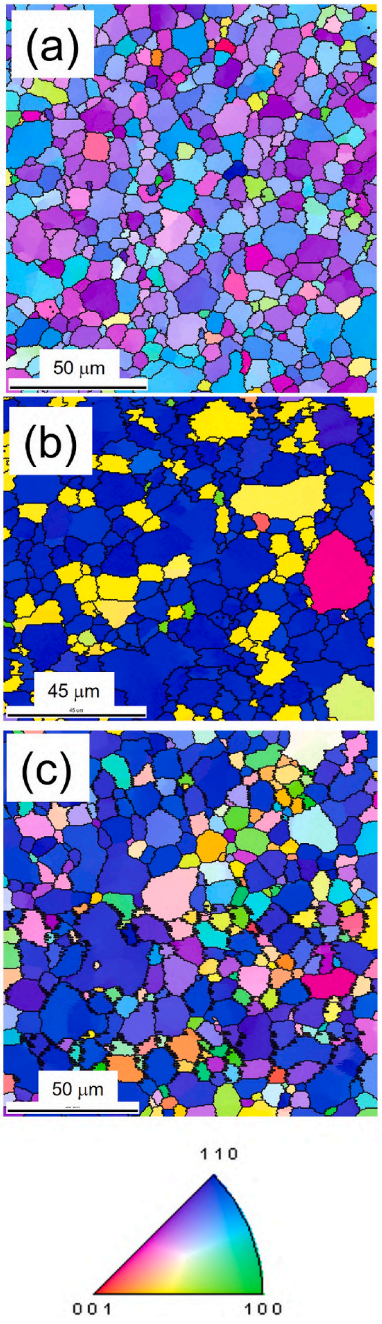

Fig. 5. Plan-view EBSD showing the surface orientation of Sn grains on (a) randomly-, (b) <111>–, and (c) <100>-oriented Cu substrates after 7944-h storage.

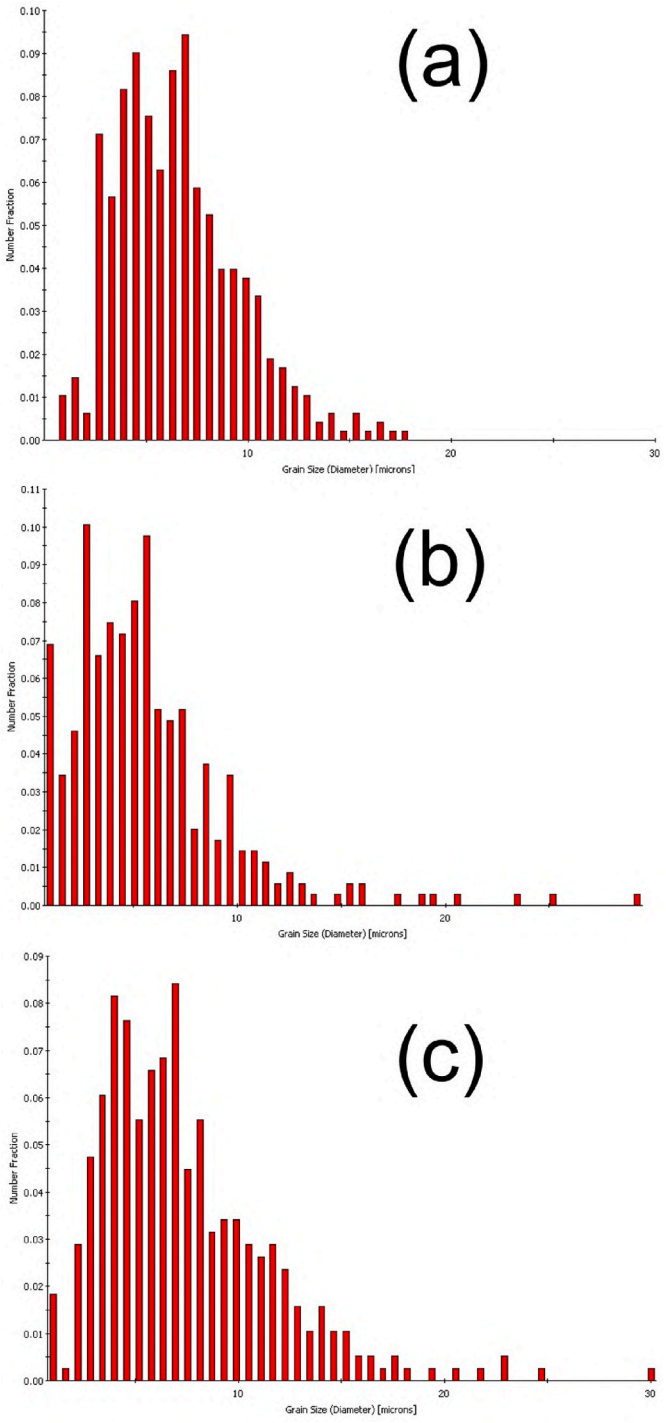

Fig. 6. Statistics of distribution of Sn grain orientation on (a) randomly-, (b) <111>−, and (c) <100>-oriented Cu substrates.

of adjacent grain boundaries were also examined. Fig. 7 presents the statistical results of misorientation angles. The Sn grains on the RO-Cu have the lowest fraction of low angle grain boundaries (0°–15°).

It is noteworthy to point out that the twin structures in the three Cu substrates are different. As shown in Fig. 1, the randomly-oriented Cu possesses micron-scale dense twins on its surface. On the other hand, for the <111>− and <100>-oriented Cu substrates, twin structures are sparse on their surface. Yet, the <111>-oriented Cu has dense nano-twinned structure beneath its surface, as presented in Fig. 4. How these twin structures affect the diffusion of Sn atoms during Cu–Sn reactions is an interesting subject. To the best of our knowledge, these twins might

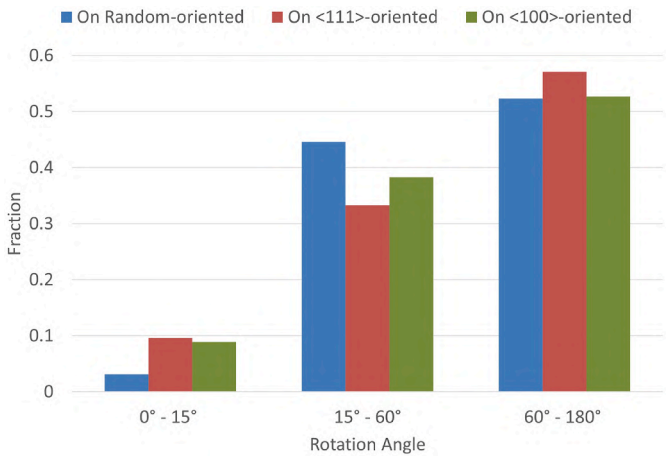

Fig. 7. Analysis of misorientation of Sn grain boundaries for the three specimens in this study.

not affect the interfacial Cu–Sn reactions.

The orientation relationship of the Sn and the Cu grains were also investigated by cross-sectional EBSD. Fig. 8 shows the orientation of the Sn grains grown on the RO-Cu films. The Sn grains possess a moderate preferred orientation of <221>, which is consistent with the results from plan-view analysis in Fig. 5. Most of the Sn grains are bamboo-like structures. The RO-Cu beneath it has no obvious preferred orientation. Fig. 9 presents the orientation of Sn grains and the <111> Cu films, from which the Sn grains grew. The Sn grains have a strong <110> texture, and the Cu grains possess a strong <111> texture. For the Sn grains on <100> Cu, they also have a strong <110> orientation, as illustrated in Fig. 10. On the other hand, the <100> Cu has a very large grain size, and it has a very strong <100> texture. The above results indicate the orientation of the Cu films has a big influence on the orientation of the immersion Sn grains. The above results imply that the orientation of the Sn grains may play an important role in formation of CuSn IMCs, and thus affect the growth of Sn whiskers.

The orientation relationship between the Sn whisker and the parent Sn grain is also examined. Fig. 11 depicts the enlarged plan-view SEM image for the Sn whiskers in Fig. 3(d). Many whiskers grew from the Sn grains on RO-Cu film after aging at room temperature for 7944 h. Their diameters range from a few to ten microns. We prepared a cross-section of a Sn whisker on a Sn parent grain, and analyzed the orientation relationship between the two grains by EBSD. The results are presented in Fig. 12, and the lattice cells of Sn grains are also labeled. One can observe that the orientation of the Sn whisker grain is almost identical to that of the parent Sn grain, with only few degrees of misorientation. This misorientation may be attributed to that the Sn whisker may bend after growing from the parent Sn grain.

The effect of these specifically-oriented Cu films on Sn–Cu interaction was not clear. However, they did show a great influence on altering the diffusion mechanism between Cu and Sn at lower temperature. There is a phenomenon called surface segregation. Surface segregation is about the enrichment of one component on the surface of an alloy [60,61]. There are some investigations on surface segregation between Sn and single crystal Cu, especially focused on the low-indexed plane, such as (111), (100) and (110) [62,63]. The results showed that Sn atoms tend to segregate on well-defined surface orientations and form an ordered structure. In 2005, Asante et al. [64] studied the surface segregation of Sn in Cu single crystals with AES (Auger electron spectroscopy). They summarized their work and concluded that the segregation parameters of Sn, including the diffusion coefficient D, the segregation energy ΔG, and interaction energy $\Omega_{Cu–Sn}$:

$D_{(111)} = 9.2 \times 10^{-4} \exp(-205/RT)\ m^2\ s^{-1}$; $\Delta G_{(111)} = 70\ kJ\ mol^{-1}$; $\Omega_{Cu–Sn} = 3.8\ kJ\ mol^{-1}$

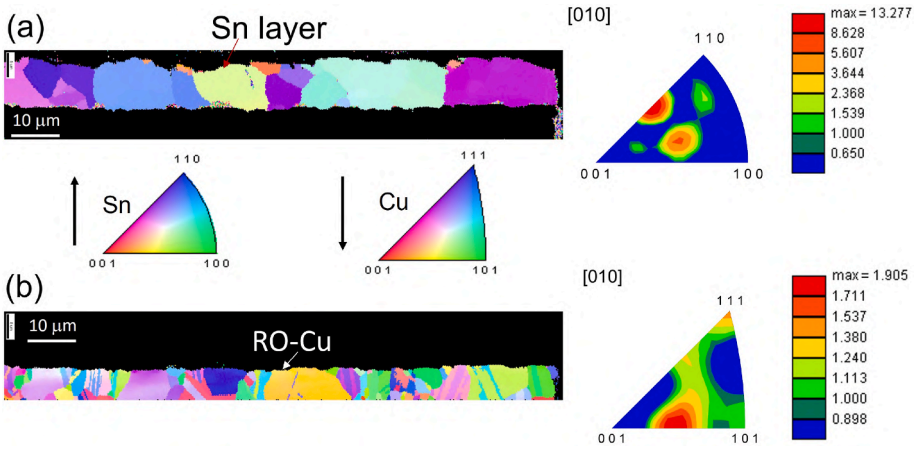

Fig. 8. Cross-sectional EBSD showing the orientations of the Sn grains on the RO-Cu film. (a) Orientation of the Sn layer. There is a preferred orientation close to <221>. (b) Orientation of the Cu film beneath the Sn layer.

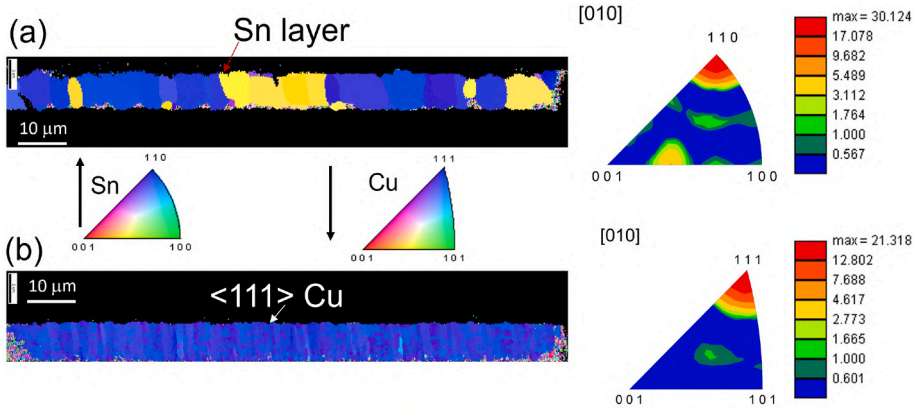

Fig. 9. Cross-sectional EBSD showing the orientations of the Sn grains on the <111>-Cu film. (a) Orientation of the Sn layer. There is a preferred orientation of <110>. (b) Orientation of the Cu film beneath the Sn layer, and it has a <111> preferred orientation.

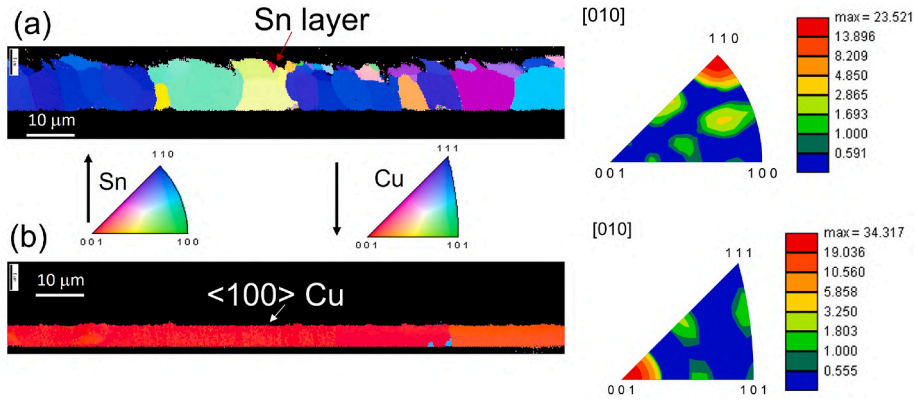

Fig. 10. Cross-sectional EBSD showing the orientations of the Sn grains on the <100>-Cu film. (a) Orientation of the Sn layer. There is a <110> preferred orientation. (b) Orientation of the Cu film beneath the Sn layer, and it has a <100> preferred orientation.

$D_{(100)} = 6.2 \times 10^{-6} \exp(-189/RT)\ m^2\ s^{-1}$; $\Delta G_{(100)} = 65\ kJ\ mol^{-1}$; $\Omega_{Cu-Sn} = 3.9\ kJ\ mol^{-1}$

With such a high diffusivity on (111) and (100) planes, the diffusion of Cu atoms along grain boundaries of Sn is no longer dominating in the diffusion couple. Sn atoms on specifically-oriented Cu films are likely to spread out and cover the surface of Cu. Because the formation of Cu_6Sn_5 is a diffusion-controlled process, the morphology of Cu_6Sn_5 can be expected to be uniform and flat on <111>– and <100>-oriented Cu. In addition, it is reported that the different Cu surface orientation significantly affects the morphologies and the orientation of Cu_6Sn_5 interfacial IMCs, which is mainly attributed to the lattice mismatch between the Cu surface grain and the Cu_6Sn_5 grain [49]. Therefore, different morphologies of Cu_6Sn_5 IMCs may impose different strain in the Sn grains, and affect the whisker growth rate.

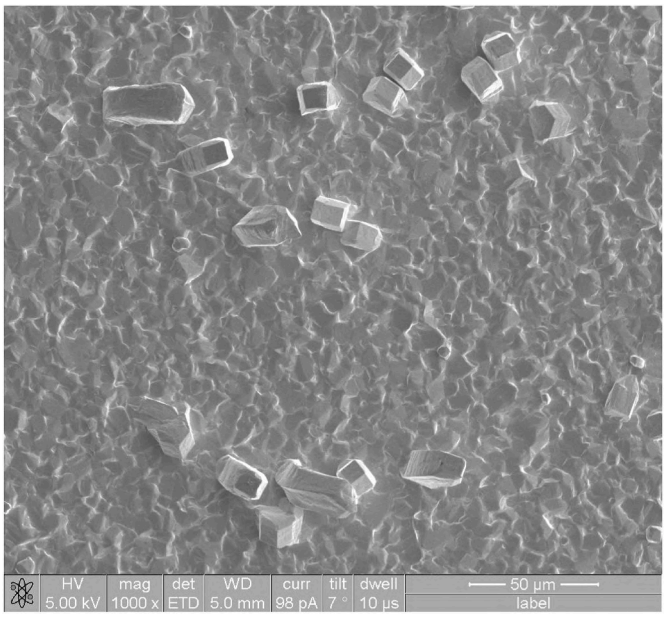

Fig. 11. Plan-view FIB electron image at a higher magnification showing Sn whiskers on a randomly-oriented Cu substrate after 7944-h RT storage.

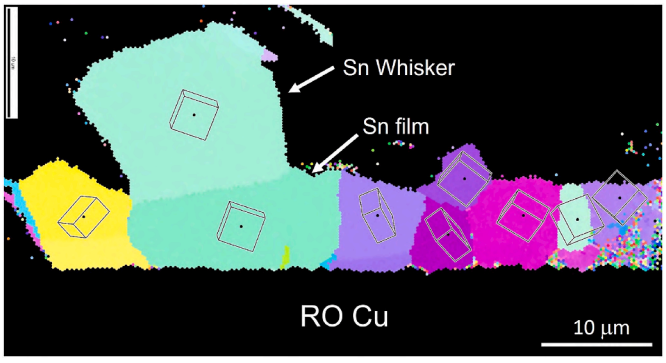

Fig. 12. Cross-sectional EBSD image showing the orientation relationship between a Sn whisker and its parent Sn grain on a randomly-oriented Cu substrate after 7944-h RT storage.

However, based on this assumption, the <111>-oriented Cu should have a better performance on relieving whisker formation, because it has a higher diffusivity. However, in this study, the grain size of <111>− and <100>-oriented Cu is quite different. The grain size of <111>-oriented Cu is 1.04 μm, and that of <100>-oriented Cu was 369.97 μm. We believed that the smaller grain size of <111>-oriented Cu would reduce its effect on distributing Sn atoms. There are more boundaries that need to be stepped across as Sn atoms diffuse on <111> plane. The efficiency of <100>-oriented Cu on retarding whiskers is benefited from not only its specifically-oriented texture, but also on its surface in the giant grain structure.

4. Conclusion

In summary, we examined the effect of crystallographic orientation of Cu substrates on the growth of Sn whiskers. The whiskers grew on pure Sn layers electroplated on randomly-oriented Cu after weeks of RT storage. In contrast, there was no extrusion found on the Sn layers with <111>-oriented Cu underlays until 1200 h of storage. The effect of <100>-oriented Cu films was even better, not having any extrusions for 7944 h. It is noticeable that even though some whiskers were found on the Sn layers with specifically-oriented Cu, they were quite small and short.

The mechanism of relieving whisker formation is established on controlling the behavior of IMC formation. Both Sn and Cu orientations may play key roles in the formation of the Cu–Sn IMCs. The Sn grains on both <111>− and <100>-oriented Cu have a strong <110> texture. The Cu_6Sn_5 would be formed more evenly on the <111>− and <100>-oriented Cu, giving less concentrated compressive stress distribution. The unique interaction between the Sn layer and the specifically-oriented Cu films is not clear. Further studies are required to investigate how it works. However, surface segregation of Sn atoms on the surface of <111>− and <100>-oriented Cu might be a possible explanation to this special phenomenon.

Declaration of competing interest

The authors declare that they have no known competing financial interests or personal relationships that could have appeared to influence the work reported in this paper.

Acknowledgments

This work was financially supported by the National Science and Technology Council, Taiwan, T-Star center project “Future Semiconductor Technology Research Center”, under Grant No. NSTC 113-2634-F-A49-008 and No. NSTC 96-2628-E-009 -010 -MY3

References

[1] Compton K, Mendizza A, Arnold S. Filamentary growths on metal surfaces–“whiskers”. Corrosion 1951;7(10):327–34.
[2] Zhang L, Xiong D, Su Z, et al. Molecular dynamics simulation and experimental study of tin growth in SAC lead-free microsolder joints under thermo-mechanical-electrical coupling. Mater Today Commun 2022;33:104301.
[3] Tian Z, Zhang P, Zhang Y, et al. Tin whisker growth from titanium-tin intermetallic and the mechanism. J Mater Sci Technol 2022;129:79–86.
[4] NASA whisker failures: https://nepp.nasa.gov/whisker/failures/acceced on 22 December 2024.
[5] Glazunova V. A study of the influence of certain factors on the growth of filamentary tin crystals. Kristallografiya 1962;7(5):761–8.
[6] Lindborg U. Observations on the growth of whisker crystals from zinc electroplate. Metall Trans A 1975;6:1581–6.
[7] Lindborg U. A model for the spontaneous growth of zinc, cadmium and tin whiskers. Acta Metall 1976;24(2):181–6.
[8] Vianco P, Cummings D, Kotula P, et al. Mitigation of long whisker growth based upon the dynamic recrystallization mechanism. J Electron Mater 2020;49:888–904.
[9] Tu K-N. Interdiffusion and reaction in bimetallic Cu-Sn thin films. Acta Metall 1973;21(4):347–54.
[10] Tu K-N. Irreversible processes of spontaneous whisker growth in bimetallic Cu-Sn thin-film reactions. Phys Rev B 1994;49(3):2030.
[11] Lee B-Z, Lee D. Spontaneous growth mechanism of tin whiskers. Acta Mater 1998;46(10):3701–14.
[12] Illés B, Krammer O, Hurtony T, et al. Kinetics of Sn whisker growth from Sn thin-films on Cu substrate. J Mater Sci Mater Electron 2020;31:16314–23.
[13] Jagtap P, Sethuraman VA, Kumar P. Critical evaluation of relative importance of stress and stress gradient in whisker growth in Sn coatings. J Electron Mater 2018;47:5229–42.
[14] Subramanian K, Tu K, Chen C, et al. Stress analysis of spontaneous Sn whisker growth. Lead-free electronic solders: a special issue of the journal of materials science. Mater Electron 2007:269–81.
[15] Chason E, Jadhav N, Chan W, et al. Whisker formation in Sn and Pb–Sn coatings: role of intermetallic growth, stress evolution, and plastic deformation processes. Appl Phys Lett 2008;92(17).
[16] Sobiech M, Wohlschlögel M, Welzel U, et al. Local, submicron, strain gradients as the cause of Sn whisker growth. Appl Phys Lett 2009;94(22).
[17] Pei F, Jadhav N, Chason E. Correlating whisker growth and grain structure on Sn-Cu samples by real-time scanning electron microscopy and backscattering diffraction characterization. Appl Phys Lett 2012;100(22).
[18] Pei F, Chason E. In situ measurement of stress and whisker/hillock density during thermal cycling of Sn layers. J Electron Mater 2014;43:80–7.
[19] Jagtap P, Jain N, Bower A, et al. Sn whisker growth during mechanical loading and unloading: highlighting the critical role of stress in whisker growth. J Electron Mater 2023;52(2):773–81.
[20] Vjpra Karpov. Electrostatic theory of metal whiskers. Phys Rev Appl 2014;1(4):044001.
[21] Borra V, Georgiev DG, Karpov V, et al. Microscopic structure of metal whiskers. Phys Rev Appl 2018;9(5):054029.

[22] Karpov VG. Understanding the movements of metal whiskers. J Appl Phys 2015; 117(23).
[23] Niraula D, McCulloch J, Warrell G, et al. Electric field stimulated growth of Zn whiskers. AIP Adv 2016;6(7).
[24] Subedi B, Niraula D, Vgjapl Karpov. The stochastic growth of metal whiskers 2017; 110(25).
[25] Vasko AC, Grice CR, Kostic AD, et al. Evidence of electric-field-accelerated growth of tin whiskers. MRS Communications 2015;5:619–22.
[26] Zhang Q, Tian Z, Zhang P, et al. Rapid and massive growth of tin whisker on mechanochemically decomposed Ti2SnC. Mater Today Commun 2022;31:103466.
[27] Tang H, Yan B, Zhang P, et al. Controlling tin whisker growth via oxygen-mediated decomposition of Ti2SnC, vol. 59; 2024. p. 1958–67.
[28] Zhang L, Li J, Xiong D, et al. Dynamic growth mechanism of tin whisker driven by compressive stress under thermal-mechanic-electric-diffusion coupling. Vacuum 2023;215:112299.
[29] Sun M, Dong M, Wang D, et al. Growth behavior of tin whisker on SnAg microbump under compressive stress. Scr Mater 2018;147:114–8.
[30] Hashim AN, Salleh MAAM, Ramli MM, et al. Effect of isothermal annealing on Sn whisker growth behavior of Sn0. 7Cu0. 05Ni solder joint. Materials 2023;16(5): 1852.
[31] Fukuda Y, Osterman M, Pecht M. The impact of electrical current, mechanical bending, and thermal annealing on tin whisker growth. Microelectron Reliab 2007; 47(1):88–92.
[32] Zhang X, Yang C, Sun M, et al. Inhibition of tin whisker by electroplating ultra-thin Co-W amorphous barrier layer. Mater Char 2020;162:110221.
[33] Yang L, Qiao J, Zhang Y, et al. Effects of rare earth Ce addition on the microstructure and shear property of Cu/In-50Ag/Cu composite solder joint. Microelectron Reliab 2021;127:114385.
[34] Kutilainen T, Pudas M, Ashworth MA, et al. Atomic layer deposition (ALD) to mitigate tin whisker growth and corrosion issues on printed circuit board assemblies. J Electron Mater 2019;48:7573–84.
[35] Shan Z, Lin K, Hu A, et al. Mitigation and mechanism of tin whisker on micro-bumps by hard and soft underfills. Electron Mater Lett 2022;18(6):547–58.
[36] Mahapatra SD, Dutta I. Co-electrodeposition of tin with 0.2–20% indium: implications on tin whisker growth 2018;337:478–83.
[37] Buchanan JD, Borra V, Islam MM, et al. Tin whisker growth suppression using NiO sublayers fabricated by dip coating. Condensed Matter 2022;7(1):7.
[38] Sivakumar P, Du SM, Selter M, et al. Long-term thermal aging of parylene conformal coating under high humidity and its effects on tin whisker mitigation. Polym Degrad Stab 2021;191:1–14. 109667.
[39] Hada Y, Morikawa O, Togami H. In: Proceedings of the 26th Relay Conference. Nat. Assoc. Relay Manufacturers; 1978. 9/1.
[40] Oberndorff P, Dittes M, Crema P, et al. Humidity effects on Sn whisker formation. IEEE Trans Electron Packag Manuf 2006;29(4):239–45.
[41] Schetty R. Minimization of tin whisker formation for lead-free electronics finishing. Circ World 2001;27(2):17–20.
[42] Hashim AN, Salleh MAAM, Sandu AV, et al. Effect of Ni on the suppression of Sn whisker formation in Sn-0.7 Cu solder joint. Materials 2021;14(4):738.
[43] Illés B, Choi H, Hurtony T, et al. Suppression of Sn whisker growth from SnAgCu solder alloy with TiO2 and ZnO reinforcement nano-particles by increasing the corrosion resistance of the composite alloy. J Mater Res Technol 2022;20:4231–40.
[44] Li Y, Sun M, Ren S, et al. The influence of non-uniform copper oxide layer on tin whisker growth and tin whisker growth behavior in SnAg microbumps with small diameter. Mater Lett 2020;258:126773.
[45] Majumdar B, Dutta I, Bhassyvasantha S, et al. Recent advances in mitigation of whiskers from electroplated tin. JOM 2020;72:906–17.
[46] Fadil NA, Yusof SZ, Abu Bakar TA, et al. Tin whiskers' behavior under stress load and the mitigation method for immersion tin surface finish. Materials 2021;14(22): 6817.
[47] Zhang Q, Tang J, Tang H, et al. Method for inhibiting Sn whisker growth on Ti2SnC 2022;57(43):20462–71.
[48] Tang H, Yin X, Zhang P, et al. Inhibition of whisker growth by crafting more decomposition-resistant Ti2SnC MAX phase through vanadium solid solution. Ceram Int 2024;50(21):43013–22.
[49] Hsiao H-Y, Liu C-M, Lin H-w, et al. Unidirectional growth of microbumps on (111)-oriented and nanotwinned copper. Science 2012;336(6084):1007–10.
[50] Liu T-C, Liu C-M, Hsiao H-Y, et al. Fabrication and characterization of (111)-oriented and nanotwinned Cu by DC electrodeposition. Cryst Growth Des 2012;12 (10):5012–6.
[51] Lu C-L, Lin H-W, Liu C-M, et al. Extremely anisotropic single-crystal growth in nanotwinned copper. NPG Asia Mater 2014;6(10).
[52] Lai J-Y, Tran D-P, Yang S-C, et al. Stress relaxation and grain growth behaviors of (111)-preferred nanotwinned copper during annealing. Nanomaterials 2023;13(4): 709.
[53] Tseng C-H, Tseng I-H, Huang Y-P, et al. Kinetic study of grain growth in highly (111)-preferred nanotwinned copper films. Mater Char 2020;168:110545.
[54] Zeng K, Tu K-N. Six cases of reliability study of Pb-free solder joints in electronic packaging technology. Mater Sci Eng R Rep 2002;38(2):55–105.
[55] Tran D-P, Lin T-W, Shie K-C, et al. Non-destructive micro analysis of electromigration failures in solder microbumps using 3D X-ray computed tomography. Mater Char 2022;194:112404.
[56] Suh J, Tu K-N, Tamura N. Preferred orientation relationship between Cu6Sn5 scallop-type grains and Cu substrate in reactions between molten Sn-based solders and Cu. J Appl Phys 2007;102(6).
[57] Tran D-P, Liu Y-T, Chen C. Effects of Cu/SnAgCu powder fraction and sintering time on microstructure and mechanical properties of transient liquid phase sintered joints. Materials 2024;17(9):2004.
[58] Tu K-N. Solder joint technology. Springer; 2007.
[59] Mo C-C, Tran D-P, Juang J-Y, et al. Effect of intermetallic compound bridging on the cracking resistance of Sn2. 3Ag microbumps with different UBM structures under thermal cycling. Metals 2021;11(7):1065.
[60] Wynblatt P, Ku R. Surface energy and solute strain energy effects in surface segregation. Surf Sci 1977;65(2):511–31.
[61] Barnett R, Landman U, Cleveland C. Surface segregation in simple metal alloys: an electronic theory. Phys Rev B 1983;28(12):6647.
[62] Erlewein J, Hofmann S. Segregation of tin on (111) and (100) surfaces of copper. Surf Sci 1977;68:71–8.
[63] Overbury S, Ku Y-S. Formation of stable, two-dimensional alloy-surface phases: Sn on Cu (111), Ni (111), and Pt (111). Phys Rev B 1992;46(12):7868.
[64] Asante J, Terblans J, Roos W. An AES study of Sn surface segregation in Cu single crystals. Surf Interface Anal 2005;37(5):517–21.